# Analysis of a Gap Dryer Used to Produce Polymer Films and Coatings

**Narayan Ramesh and J. L. Duda**
Center for the Study of Polymer Solvent Systems, Dept. of Chemical Engineering, Pennsylvania State University, University Park, PA 16802

*The ability to predict the drying behavior of thin films and coatings is of great importance to the coating industry and governs the economical production of various polymeric products. In conventional drying processes, a continuous layer of polymer solution is deposited onto a substrate, which is dried in an oven with forced air convection. Recently, a gap dryer was developed that eliminates the need for forced gas flow and provides direct solvent recovery. A model that incorporates simultaneous heat and mass transfer in the bulk polymer and gas phases and jump conditions across the interface is utilized to describe the drying of a binary polymer–solvent system in a gap dryer. Solvent self-diffusion in the polymer phase is described by the free-volume theory, and the Flory-Huggins theory is used to describe polymer–solvent thermodynamics. Simulations indicate the possibility of condensation in the gas phase that can decrease both drying efficiency and coating quality. A method to resolve this problem is proposed, as well as a comparison between the performance of a gap dryer and a conventional convection-oven dryer.*

## Introduction

The efficient and economical production of polymeric films depends on the drying of solvent-coated polymer films. Polymeric coatings are typically produced by casting a continuous layer of polymer solution, comprising one or more solvents and one or more polymers onto a moving substrate and drying this coating in a convection oven dryer. Since drying determines the quality of the final product, it is of considerable importance. In many cases, nonuniformities, phase separation, and defects in the final product are attributable to poorly chosen drying conditions. A combination of experiment and theory is therefore crucial to understanding the relationship between the quality of a coating and the drying conditions chosen.

Several models exist in literature to describe the drying of a binary polymer–solvent mixture. In earlier studies, the drying process was modeled as an unsteady-state diffusion process; however, the effects of evaporative cooling and film shrinkage were neglected (Blandin et al., 1987; Waggoner and Blum, 1989). More complete models accounting for the moving boundary, unsteady-state heat and mass transfer, and diffusion-induced convection have been developed. In one such study, drying of polyvinyl alcohol in water has been considered from both a theoretical and experimental perspective. The effect of diffusion and convective mass transfer, heat transfer to the film, and movement of the boundary have been considered (Okazaki, 1974). The model also incorporates unequal polymer and solvent densities, assuming that the volume of the polymer and solvent are additive at all compositions. In another study, a model is presented to describe coating of any number of components on a base stock (Yapel, 1988). The model is formulated based on the volume additivity of the two components and the temperature profile in the substrate, and coatings are solved by considering the unsteady-state heat-transfer problem. Effects of convective heating and evaporative cooling have also been included. The temperature and concentration dependence of the diffusion coefficient has been described by the free-volume theory (Vrentas and Duda, 1977a,b). In the studies conducted by Yapel and Okazaki, the mass average velocity was used to analyze mass transfer in the polymer film. The advantage of using a volume-average velocity in analyzing the mass-transfer problem has been pointed out in later studies (Vrentas

Correspondence concerning this article should be addressed to .

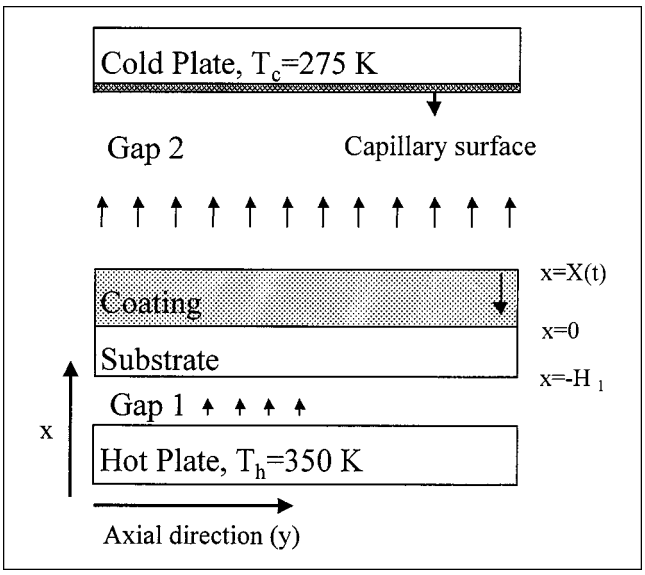


**Figure 1. The gap dryer and drying geometry.**

Drying occurs in the direction of the *x*-axis, while the axial direction, the *y*-axis, is along the length of the dryer. The *z*-axis (width) goes into the plane of the paper.

and Vrentas, 1994a; Cairncross et al., 1992). Cairncross and coworkers have modeled a dryer where radiant and convective heat transfer are important, and also analyzed the formation of blisters in coatings (Cairncross et al., 1995). Vrentas and Vrentas have shown the utilization of jump balances in the formulation of the problem (Vrentas and Vrentas, 1994a). Price et al. followed the formulation of Vrentas and Vrentas, and used drying experiments to correlate diffusion behavior in polymer–solvent systems (Price et al., 1997).

Most often, dryers used in industry are forced-convection dryers, where hot air is blown across the film to evaporate the solvent. Recently, a gap dryer has been developed that eliminates the need for forced convection and facilitates direct solvent recovery (Huelsman and Kolb, 1997). As a consequence, detrimental environmental effects from volatile organic compounds escaping into the atmosphere are avoided. A detailed description of a gap dryer is provided in the next section. In this work, a model has been developed to describe the drying process in a gap dryer. Some aspects of the model are based on drying studies conducted to describe the drying process in a convection oven dryer (Vrentas and Vrentas, 1994a; Alsoy and Duda, 1998). Since the mechanism of heat and mass transport in a gap dryer is different from a convection oven dryer, appropriate modifications have been made to incorporate these differences.

## Gap Dryer

A gap dryer (shown in Figure 1) is a device used for drying polymer coatings; it eliminates the need for forced gas flow and provides direct solvent recovery (Huelsman and Kolb, 1997). Forced gas flow is eliminated in a gap dryer by having a hot plate and a cold plate separated by a small gap (Kolb and Huelsman, 1998). The hot plate is located adjacent to the substrate and provides energy to evaporate the solvent. The cold plate is positioned adjacent to the coating and provides a driving force for solvent vapor transport across the gap. The hot plate supplies energy, and the driving force for mass transfer is the difference in concentration of the solvent at the hot polymer surface and the cold plate. The cold plate is provided with a surface geometry that prevents the liquid from dripping back onto the coated surface and transports the coated solvent from the plate into a collection device (Huelsman and Kolb, 1997). The dimensions of gap 1 vary (see Figure 1), and it is advantageous to have the smallest gap that can be maintained without the two plates touching. A typical value may be around 140 microns. Gap 2 is bigger and may be between 0.15 and 5 cm wide (Huelsman and Kolb, 1997). The size of gap 2 is dictated by physical considerations of how small a gap can be maintained. While a smaller size for gap 2 is preferable, the load on the cooling system is increased as gap 2 becomes smaller. The temperatures of the hot plate and cold plate are dictated by the specific polymer–solvent system, the residual solvent level desired, and the initial conditions such as the temperature of the coating and concentration of the solvent in the coating. Drying and solvent recovery proceed simultaneously as the solvent is transported across gap 2.

The bottom surface of the cold plate is the condensing surface and has transverse open channels or grooves. Capillary forces prevent the liquid from dripping back onto the coating by gravity and transport the condensed solvent laterally to the edges. When the liquid contacts the end of the grooves between the edge plates and the condensing surface, a liquid meniscus forms and creates a low-pressure surface that draws the condensate from the condensing surface laterally to the collection device. Gravity overcomes capillary forces in the meniscus and liquid flows as a film down the face of the edge plate to a suitable collection device (Kolb and Huelsman, 1998). The grooves can be triangular, rectangular, or circular, or other complex shape. The key design aspects in solvent recovery are choice of groove material, geometry, and dimensions that are dictated by the drying rate and physical properties of the condensate (Huelsman and Kolb, 1997).

One of the advantages of a gap dryer over the more commonly used convection-oven dryer is that large volumes of heated gas are not required to evaporate the solvent. In a convection-oven dryer, the motion of air over the coating can cause mottle defects and banding. In order to avoid mottling and banding, the air velocity must be reduced, which in turn reduces the drying rate (Kolb and Huelsman, 1998). Limitations of the gap dryer are that small gaps place a greater load on the cooling system, and since heat transfer is faster than mass transfer, condensation can occur in the gas phase, destroying the efficiency of the drying process.

## Assumptions

The model developed in the next section incorporates aspects such as movement of the boundary, evaporative cooling, heat transfer to and from the polymer phase, and heat and mass transfer in the gas phase. Jump conditions are used to describe the heat and mass transfer at the polymer–gas interface. The strong temperature and concentration dependence of diffusivity in the polymer phase is described us-

ing the free-volume theory of transport (Vrentas and Duda, 1977a,b). The problem is formulated in volume-average terms to eliminate the convection term in the polymer phase. The boundary has been immobilized through a transformation to avoid complications involved in formulating finite difference grids. Gradients in the axial direction and along the width of the coating are neglected, consequently a one-dimensional problem is treated. In the solution to this problem, one spatial element is followed in time, starting from the initial conditions at $t = 0$. The temperature and concentration values obtained as a function of time reflect the progress of the drying process. In this study, all the equations are formulated by considering a binary polymer–solvent system.

The drying geometry is shown in Figure 1. Initially, the polymer film has a constant thickness, $L$, and extends from $x = 0$ to $x = X(t = 0)$. In a typical drying operation, the polymer solution is cast on a substrate belt of constant thickness $H_1$, and the substrate moves through the dryer. The temperature of the hot plate is $T_h$, and the temperature of the cold plate is $T_c$. Based on this geometry, the assumptions used to formulate the model are listed below.

1. Gradients in concentration and temperature along the width of the coating ($z$-direction) are neglected, since the width of the slab is much greater than the thickness.
2. Axial ($y$-axis) conduction and axial diffusion are negligible.
3. Complications that can arise as a result of drag on the polymer film by the gas phase are neglected.
4. The gas phase is treated as ideal to obtain the concentration and mol fraction from partial pressures.
5. Radiative heat transfer has been included in the formulation of the model, and the view factors in both gap 1 and gap 2 are assumed to be 1.
6. The heat-transfer processes can be adequately described using constant values of density, heat capacity, and thermal conductivity for the coating and substrate.
7. The polymer and solvent can have different partial specific volumes; however, they are not a function of the composition of the system. It is also assumed that average values of the specific volumes can be used in the temperature range of interest to formulate the problem.
8. The resistance to heat transfer lies predominantly in the gas phase; therefore, a single uniform temperature for the polymer film and substrate layer is assumed (Vrentas and Vrentas, 1994a).
9. The kinetic energy exchange at all interfaces is negligible.
10. The temperature is above the glass transition temperature of the polymer–solvent mixture throughout the drying process.
11. The coating and substrate move at a low enough velocity so that a significant enhancement in the heat-transfer coefficient does not occur. The mass-transfer process also remains unaffected by the movement of the substrate.
12. The gas-phase mass-transfer process can be characterized by a constant value of diffusivity since the gas-phase diffusivity is a weak function of temperature.
13. The total pressure in the gas phase is essentially constant.
14. It is assumed that pseudo-steady-state conditions are good approximations for the heat-transfer process in gap 1, gap 2, and the coating, and for the mass-transfer process in the gas phase, since the drying process is primarily controlled by mass transfer in the polymer phase. Consequently, heat and mass transfer in the gas phase and heat transfer in the polymer and substrate are fast compared to the mass transfer in the polymer phase (Vrentas and Vrentas, 1994a).
15. The solvent does not penetrate the substrate.

## Equations and Dimensionless Variables

Based on previous drying models that exist in the literature and the assumption tabulated in the previous section, equations describing the drying process are formulated (Vrentas and Vrentas, 1994a; Alsoy and Duda, 1998).

The species continuity equation for the solvent in the polymer is given by

$$\frac{\partial \rho_s^c}{\partial t} = \frac{\partial}{\partial x}\left( D \frac{\partial \rho_s^c}{\partial x} \right). \tag{1}$$

Here, $\rho_s^c$ denotes the concentration of the solvent in the polymer film, and $D$ is the mutual binary diffusion coefficient. The mutual binary diffusion coefficient, $D$, is a function of temperature and concentration. The self-diffusion coefficient, $D_1$, for the solvent in the polymer is obtained using the free-volume theory of transport, which has been shown to accurately correlate and predict the solvent self-diffusion coefficients in polymeric systems (Vrentas and Duda, 1977a,b). The expression for the self-diffusion coefficient is given below:

$$D_1 = D_{01} \exp(-E/RT) \exp\left\{ -\left( \omega_1 \hat{V}_1^* + \omega_2 \zeta \hat{V}_2^* \right) / \left( \hat{V}_{FH}/\gamma \right) \right\}. \tag{2}$$

In Eq. 2, $D_{01}$ is the preexponential factor, $\omega_1$ and $\omega_2$ are the solvent and polymer weight fractions, $\zeta$ is the ratio of the molar volume of the jumping unit of the solvent to that of the polymer, $\hat{V}_1^*$ and $\hat{V}_2^*$ are the specific volumes of the jumping units of the solvent and polymer, respectively, and $\hat{V}_{FH}/\gamma$ is the free-volume of the system. Also, $E$ is the energy required for solvent molecules to escape from their neighbors, $R$ is the gas constant, and $T$ is the temperature. It is assumed that the free volume of the system can be obtained by the addition of the free volumes of the polymer and solvent and is given by the following relation:

$$\frac{\hat{V}_{FH}}{\gamma} = \omega_1 \frac{K_{11}}{\gamma_1}\left( K_{21} - T_{g1} + T \right) + \omega_2 \frac{K_{12}}{\gamma_2}\left( K_{22} - T_{g2} + T \right). \tag{3}$$

In the preceding equation, $K_{11}$ and $K_{21}$ are the free-volume parameters for the solvent, while $K_{12}$ and $K_{22}$ are the free-volume parameters for the polymer; and $T_{g1}$ and $T_{g2}$ are the glass transition temperature of the solvent and polymer, respectively.

The Flory-Huggins theory is utilized to obtain the mutual binary diffusion coefficient from the self-diffusion coefficient. This formulation is extremely useful for predicting the mu-

tual binary diffusion coefficient above the glass transition temperature, and the expression for the mutual binary diffusion coefficient is given below:

$$D = D_1(1-\phi_1)^2(1-2\chi\phi_1). \tag{4}$$

In Eq. 4, $\phi_1$ and $\chi$ are the volume fraction of the solvent in the polymer and the Flory-Huggins interaction parameter, respectively.

Techniques have been developed so that all the parameters in Eqs. 2, 3, and 4 can be estimated from properties of the two pure components making up the mixture (Zielinski and Duda, 1992b; Vrentas and Vrentas, 1994b; and Vrentas and Vrentas, 1998).

The initial composition of the solvent in the polymer phase is assumed to be uniform:

$$\rho_s^c(t=0,x) = \rho_s^o. \tag{5}$$

A no-flux boundary condition is imposed at the substrate-polymer interface since it is assumed that the substrate does not absorb any solvent. The second boundary condition resulting from a solvent jump balance at the polymer–gas interface is one of equality of fluxes in the polymer and gas phases. The boundary conditions are given below:

$$\frac{\partial \rho_s^c}{\partial x} = 0 \qquad \text{at} \quad x = 0 \tag{6}$$

$$-D\frac{\partial \rho_s^c}{\partial x} - \rho_s^c\frac{dX(t)}{dt} = n_s^g \qquad \text{at} \quad x = X(t). \tag{7}$$

In the preceding equations, $n_s^g$ is the flux of the solvent in the gas phase, $X(t)$ is the position of the polymer–gas interface, and $\rho_s^o$ is the is the initial concentration of the solvent in the coating. Equation 8 relates the polymer and solvent fluxes in volume-average coordinates, and is given by

$$(j_p^c)\hat{V}_p + (j_s^c)\hat{V}_s = 0. \tag{8}$$

In the preceding equation, $j_p^c$ and $j_s^c$ are the polymer and solvent fluxes in volume-average coordinates, and $\hat{V}_s$, $\hat{V}_p$ are the partial specific volumes of the solvent and polymer, respectively.

While the initial thickness of the coating is $L$, as the solvent evaporates, the gas–polymer interface moves. The movement of this boundary is given by Eq. 9, which is obtained from a polymer jump mass balance in conjunction with Eq. 8 and recognizing that the sum of the volume fraction of the polymer and solvent equals 1:

$$\frac{dX(t)}{dt} = \frac{D\hat{V}_s}{1-\rho_s^c\hat{V}_s}\frac{\partial \rho_s^c}{\partial x} \tag{9}$$

$$X(t=0) = L. \tag{10}$$

The initial temperature in the slab is assumed to be uniform

$$T(t=0) = T_o. \tag{11}$$

The jump energy balance across the entire slab has been derived previously (Vrentas and Vrentas, 1994a). Following the same approach and incorporating the radiation term and heat transfer by conduction, the expression for the time dependence of temperature change in the slab is obtained as

$$\frac{dT}{dt} = \frac{\Delta H_{lv}\rho_p\dfrac{dX(t)}{dt} + k^{\text{air2}}\dfrac{\partial T}{\partial x}\bigg|_{X(t)} - \sigma\left(T^4 - T_c^4\right)|_{X(t)} - k^{\text{air1}}\dfrac{\partial T}{\partial x}\bigg|_{-H_1} + \sigma\left(T_h^4 - T^4\right)|_{-H_1}}{X(t)\rho_p\hat{c}_p^{\text{poly}} + H_1\rho_s\hat{c}_p^{\text{subs}}}, \tag{12}$$

where $\Delta H_{lv}$, $k^{\text{air2}}$ and $k^{\text{air1}}$ are the latent heat of vaporization of the solvent; the thermal conductivity of the gas phase in gap 2 and gap 1, respectively; $\hat{c}_p^{\text{poly}}$ and $\hat{c}_p^{\text{subs}}$ are the heat capacities of the coating and substrate, respectively; $T$ is the temperature of the polymer and substrate; $H_1$ is the thickness of the substrate; and $\sigma$ is the Stefan-Boltzman constant. In formulating the expressions for radiative heat transfer, it is assumed that the view factors in gap 1 and gap 2 are 1, since the plates are close to each other. In formulating Eq. 12, it is assumed that the temperature of the hot plate and cold plate are maintained at a constant value throughout the drying process. In addition, it must be recognized that the fast rate of heat transfer in the polymer and gas phases coupled with the fact that the resistance to heat transfer in the polymer phase is a small fraction of the overall resistance allows the simplification that results in the use of an overall energy balance to describe the heat-transfer process.

The mass flux in the gas phase is represented by the steady-state approximation for the diffusion of the solvent through a stagnant film of air; where $D_{s\text{-}g}$ is the diffusion of solvent in air, $x_s^g$ is the mol fraction of solvent, and $c_s^g$ is the concentration of the solvent in the gas phase:

$$n_s^g = -D_{s-g}\frac{1}{1-x_s^g}\frac{\partial c_s^g}{\partial x}. \tag{13}$$

The Flory-Huggins equation is used to obtain the activity of the solvent at the polymer–gas interface:

$$a = \phi_1\exp\left(\phi_2 + \chi\phi_2^2\right). \tag{14}$$

In the preceding equation, $a$ is the solvent activity at the interface and $\phi_2$ is polymer volume fractions. At the cold plate, the solvent exists at its saturation pressure, which depends on the temperature of the cold plate. Consequently, the gas-phase mass transfer occurs between concentrations calculated from partial pressures (obtained from the solvent activity) at the polymer–gas interface and the saturation pressures at the cold plate. Gas-phase concentrations are obtained from the partial pressures by treating the gas phase as ideal.

The energy-balance equation becomes

$$\frac{dT^*}{dt^*} = \frac{A\dfrac{dX^*(t)}{dt} + B\left.\dfrac{\partial T^*}{\partial x^*}\right|_{\xi=1} - C\left.\dfrac{\partial T^*}{\partial x^*}\right|_{\xi=-H1/L} - G\left[2T^{*4} + 8HT^{*3} + 12H^2T^{*2} + 8H^3T^* + H^* - I^4\right]}{X^*(t) + E} \tag{26}$$

Dimensionless variables (concentration, temperature, time, and space) are defined below, and the equations cast in a dimensionless form:

$$\rho_s^{c*} = \frac{\rho_s^c}{\rho_s^o} \tag{15}$$

$$T^* = \frac{T - T_c}{T_h - T_c} \tag{16}$$

$$t^* = \frac{D_s^o t}{L^2} \tag{17}$$

$$X^* = \frac{X}{L} \tag{18}$$

where $T_h$ and $T_c$ are the temperatures of the hot plate and cold plate, respectively; $D_s^o$ is the initial mutual binary diffusion coefficient of the solvent in the polymer, and $L$ is the initial thickness of the coating. To immobilize the boundary, the coordinate transformation given below is used:

$$\xi = \frac{x}{X(t)}. \tag{19}$$

Using the preceding dimensionless variables and the coordinate transformation, the dimensionless equations are obtained. The mass-transfer equation in the polymer phase and the boundary conditions are given below:

$$\frac{\partial \rho_s^{c*}}{\partial t^*} - \frac{\xi}{X^*}\frac{dX^*}{dt^*}\frac{\partial \rho_s^{c*}}{\partial \xi} = \frac{1}{X^{*2}}\frac{\partial}{\partial \xi}\left(Q\frac{\partial \rho_s^{c*}}{\partial \xi}\right) \tag{20}$$

$$\frac{\partial \rho_s^{c*}}{\partial \xi} = 0 \qquad \text{at} \quad \xi = 0 \tag{21}$$

$$-Q\left.\frac{\partial \rho_s^{c*}}{\partial \xi}\right|_{\xi=1} - \rho_s^{c*}(\xi=1)X^*\frac{dX^*(t)}{dt^*} = SX^* \qquad \text{at} \quad \xi = 1. \tag{22}$$

The initial condition becomes

$$\rho_s^{o*}(t=0,\xi) = 1. \tag{23}$$

The movement of the boundary is given by

$$X^*\frac{dX^*(t)}{dt} = \frac{Q\hat{V}_s}{1-\rho_s^c\hat{V}_s}\left.\frac{\partial \rho_s^{c*}}{\partial \xi}\right|_{\xi=1}. \tag{24}$$

The gas-phase flux is given by

$$n_s^{g*} = -F\frac{1}{1-x_s^g}\frac{\partial c_s^{*g}}{\partial x^*}. \tag{25}$$

The dimensionless groups arising from the analysis are

$$Q = \frac{D}{D_s^o} \tag{27}$$

$$A = \frac{\Delta H_{lv}}{(T_h - T_c)\hat{c}_p^{\text{poly}}} \tag{28}$$

$$B = \frac{k^{\text{air2}}}{D_s^o\rho_p\hat{c}_p^{\text{poly}}} \tag{29}$$

$$C = \frac{k^{\text{air1}}}{D_s^o\rho_p\hat{c}_p^{\text{poly}}} \tag{30}$$

$$E = \frac{H_1\rho_s\hat{c}_p^{\text{subs}}}{L\rho_p\hat{c}_p^{\text{poly}}} \tag{31}$$

$$F = \frac{D_{s-g}}{D_s^o} \tag{32}$$

$$G = \frac{\sigma L(T_h - T_c)^3}{D_s^o\rho_p\hat{c}_p^{\text{poly}}} \tag{33}$$

$$H = \frac{T_c}{T_h - T_c} \tag{34}$$

$$I = \frac{T_h}{T_h - T_c}. \tag{35}$$

In order to facilitate a compact representation, the pseudo-steady-state gas-phase flux, which changes with time, is nondimensionlized according to the equation given below, and it must be recognized that $S = n_s^{g*}$:

$$S = \frac{n_{s\text{-}g}L}{D_s^o\rho_s^o}. \tag{36}$$

In typical drying problems, sharp gradients exist at the polymer–gas interface. In order to avoid calculating a derivative at this interface, integrated forms of the equations describing the boundary condition and the position of the boundary are used (Vrentas and Vrentas, 1994a):

$$X^* = \frac{1-\hat{V}_s\rho_s^o}{1-\hat{V}_s\rho_s^o\int_0^1\rho_s^{c*}\,d\xi} \tag{37}$$

$$\frac{d}{dt^*}\left(X^*\int_0^1\rho_s^{c*}\,d\xi\right) = -S. \tag{38}$$

Equation 37 is obtained by integrating Eq. 20 between $\xi = 0$ and $\xi = 1$, and substituting the integrated form of this equation into Eq. 22, while Eq. 38 is obtained using the integrated form of Eq. 20 in conjunction with Eqs. 23 and 24.

## Solution Procedure

The equations of the model result in a set of nonlinear partial differential equations that are coupled. The set of coupled partial differential equations were converted into a set of nonlinear algebraic equations using an implicit finite difference scheme. As in at least one previous study (Alsoy and Duda, 1998), the resulting equations were solved using the IMSL subroutine DNEQNF. In the solution to this problem, a variable grid was used in the polymer phase, with a smaller grid size near the polymer–gas interface and larger grid intervals near the polymer–substrate interface. Details of the equations used to generate the nonuniform grid are available in the work of Alsoy and Duda (1998). To solve the gap-dryer problem, 200 grid points were used in the polymer phase and 50 grid points were used in the gas phase. For the parameters chosen to model the convection-oven dryer, 500 grid points were required in the polymer phase to resolve the sharp gradients at the polymer–gas interface. The accuracy of the simulations was checked by increasing the number of grid points in the polymer and gas phases.

## Results and Discussion

Unfortunately, the model cannot be compared to experimental measurements, since no data from a gap dryer are available in the literature. Of particular interest would be the behavior of the gap dryer compared to conventional forced-convection drying systems. Since experimental and theoretical results for the drying of polyvinyl acetate–toluene (PVAC–toluene) under forced-convection drying conditions are available in the literature (Alsoy and Duda, 1998), the model of the gap dryer was applied to the drying of that system under conditions analogous to forced-convection drying. This is also an optimum system for evaluating the gap dryer and the associated model, since the mutual binary diffusion coefficient for the toluene–PVAC system is a very strong function of concentration, which leads to sharp concentration gradients associated with surface skinning during drying. Also, detailed information concerning the concentration and temperature dependency of the diffusion coefficient, as well as the vapor–liquid thermodynamic behavior of this system, are available from previous studies (Zielinski, 1992a; Hong, 1994). To facilitate the analysis, the Flory-Huggins theory was used to relate the self-diffusion coefficient correlated with the free-volume theory to the mutual binary diffusion coefficient, as well as phase equilibrium at the polymer–vapor interface. The thermodynamic and free-volume parameters for this system were obtained from the literature (Alsoy and Duda, 1998) and are reported in Table 1. The vapor pressure of the solvent was predicted using the Antoine equation, and Antoine constants were obtained from the DIPPR Data Compilation (Daubert and Danner, 1994).

In this analysis, the characteristics of the gap dryer were based on the information given in the original patent (Huels-

**Table 1. Free Volume Parameters for PVAC–Toluene System Used to Predict Diffusivity as a Function of Temperature and Concentration**

| Parameters | Values |
|---|---|
| $D_0$ (cm$^2$/s) | 0.00825 |
| $Ea$ (J/mol) | 7,787.4 |
| $K_{11}/\gamma$ (cm$^3$/g·K) | 0.00157 |
| $K_{12}/\gamma$ (cm$^3$/g·K) | 0.000433 |
| $K_{21} - T_{g1}$ (K) | −90.5 |
| $K_{22} - T_{g2}$ (K) | −256 |
| $\hat{V}_1^*$ (cm$^3$/g) | 0.917 |
| $\hat{V}_2^*$ (cm$^3$/g) | 0.85 |
| $\zeta$ | 0.77 |
| $\chi$ | 0.393 |

**Table 2. Drying Parameters for PVAC-Toluene System in a Gap Dryer**

| Parameters for Dying Simulation | Case A | Case B | Case C | Case D |
|---|---|---|---|---|
| *Initial Conditions* | | | | |
| Temperature (K) | 300 | 300 | 300 | 300 |
| Coating thickness (cm) | 0.0254 | 0.0254 | 0.0254 | 0.0254 |
| Initial concentration of solvent (g/cm$^3$) | 0.64 | 0.64 | 0.64 | 0.64 |
| *Substrate Parameters* | | | | |
| Heat capacity (J/g·K) | 1.25 | 1.25 | 1.25 | 1.25 |
| Density (g/cm$^3$) | 1.37 | 1.37 | 1.37 | 1.37 |
| Base thickness (cm) | 0.0508 | 0.0508 | 0.0508 | 0.0508 |
| *Coating Parameters* | | | | |
| Heat capacity (J/g·K) | 1.65 | 1.65 | 1.65 | 1.65 |
| Density (g/cm$^3$) | 1.18 | 1.18 | 1.18 | 1.18 |
| Heat of vaporization (J/g) | 360 | 360 | 360 | 360 |
| *Operating conditions* | | | | |
| Gap 1 thermal conductivity (W/cm·K) | 0.00030 | 0.00030 | 0.00030 | 0.00030 |
| Gap 2 thermal conductivity (W/cm·K) | 0.00027 | 0.00027 | 0.00027 | 0.00027 |
| Temperature of hot plate (K) | 350 | 350 | 350 | 350 |
| Temperature of cold plate (K) | 275 | 275 | 275 | 275 |
| Temperature of the screen (K) | No Screen | 315 | 325 | 315 (Init.) |
| Dimension of gap 1 (cm) | 0.014 | 0.014 | 0.014 | 0.014 |
| Dimension of gap 2 (cm) | 0.16 | 0.16 | 0.35 | 0.16 |
| Diffusivity of toluene in air (cm$^2$/s) | 0.092 | 0.092 | 0.092 | 0.092 |

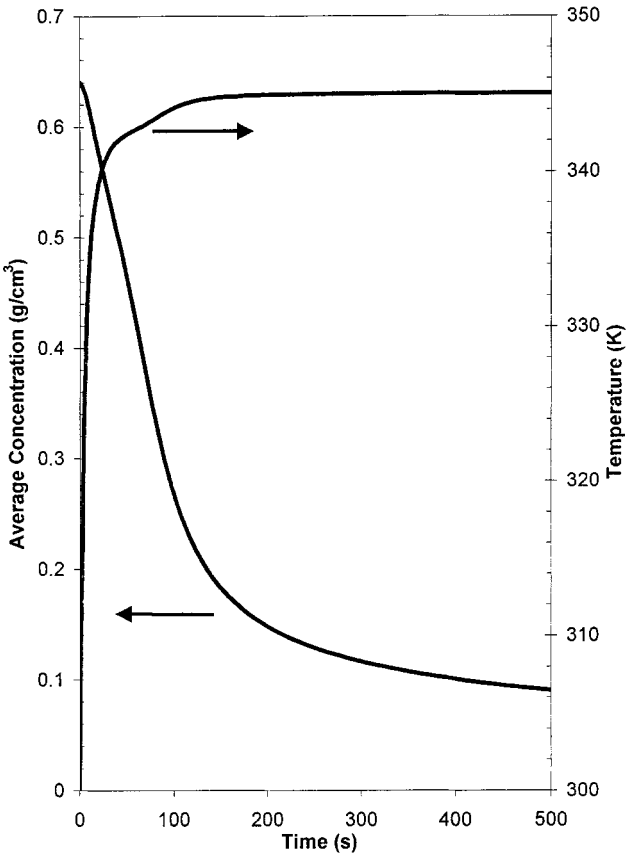


**Figure 2. Drying curve for a gap dryer without a screen for the PVAC–toluene system.**

Curves generated using the parameters given in Table 1 and Table 2 (Case A).

man and Kolb, 1997). Other parameters for the process were chosen to permit some comparison between the gap dryer and similar dryer results for the toluene–PVAC system in forced convection drying (Alsoy and Duda, 1998). All of the drying parameters used in this analysis are presented in Table 2. As this table indicates, average values for the thermal conductivity and diffusivity in the gas phase were used in the simulations, since these parameters are not strong functions of temperature. Using the system characteristics and parameters presented in Tables 1 and 2, the average concentration of toluene in the PVAC solution and the coating temperature as a function of time in the gap dryer as predicted by the model are presented in Figure 2 (Case A). From this figure, it is clear that more than 75% of the drying is complete in the first 200 s. During this initial phase of the drying process, the gas-phase mass-transfer process controls the rate of loss of solvent from the polymer solution, while the later stages of drying are controlled by the diffusion of the solvent in the coating. It should be reemphasized that in this analysis it is assumed that pseudo-steady-state conditions describe the heat and mass transfer in the gas-phase gaps during the entire drying process. Also, it was assumed that no convection in the gas phases exists either due to natural convection or drag of the moving substrate and polymer phase on the gas phase. Any such convection in the gaps would naturally lead to higher drying rates.

Exclusion of the radiation term in the analysis causes a negligible error in the concentration levels predicted by the model at early times. At long times (50 s $< t <$ 500 s), a small deviation ($< 5\%$) is observed in the predicted value of the average concentration in the slab due to radiation. The relative error grows at long times; however, the absolute error in concentration is negligible. This occurs because inclusion of the radiation term causes a lower temperature to be reached in the coating at long times. It must also be noted that for the parameters used in this model, more heat is transferred by radiation in the lower gap than is lost by radiation from the upper gap at short times, while the opposite is true at long times. Since inclusion of the radiation term does not cause a considerable change in the drying rates predicted by the model for the conditions chosen, all further discussion is limited to cases where the radiation term is excluded from the energy-balance equation.

The drying curve presented in Figure 2 (radiation not included) is qualitatively similar to drying curves that are predicted in conventional forced convection drying processes. If gap dryers can be constructed to maintain very thin gas gaps, drying rates characteristic of high-flux forced-convection dryers are attainable. A cursory analysis of the gap dryer as represented by the results in Figure 2 would indicate that the gap dryer described in the literature has the capability of competing with conventional forced-convection drying processes. However, to obtain drying rates that are competitive with conventional drying processes, large gradients in temperature and concentration are required in the upper gap. These steep gradients can lead to complications that significantly reduce the effectiveness of the gap dryer.

In the upper gap (gap 2), the vapor pressure of the solvent as well as the temperature are obviously strong functions of position in the gap. In this model, the temperature profile in gap 2 is a linear function of position. As a result, a situation can arise where the partial pressure of the solvent is greater than its saturation pressure in the gas phase and premature condensation may occur in the gas phase. This complication is associated with the fact that heat transfer is usually faster than mass transfer in the gas phase, and precondensation or fog formation has been recognized as a major problem in partial condensers (Fair et al., 1984). This behavior is illustrated in Figure 3, which shows that at the intersection of the saturation pressure curve in the gap with the actual solvent–vapor pressure curve, the region of the gas phase near the cold plate becomes supersaturated, and condensation in the gas phase will be induced. The condensed liquid–solvent droplets formed in this region would then have the tendency to rain down upon the coating. This phenomenon would significantly reduce the effective drying rate and quality of the resulting polymer film.

Analysis of the gap drying process indicates that changing the parameters for the drying process would not eliminate this potential for premature condensation in the gas phase. Decreasing the temperature gradient in the upper gap can eliminate or reduce the region of supersaturation. However, this will necessarily lead to a reduction in the drying rate and, consequently, the effectiveness of the gap drying process is considerably reduced.

As previous analyses of premature vapor-phase condensation in partial condensers have indicated, this is a very diffi-

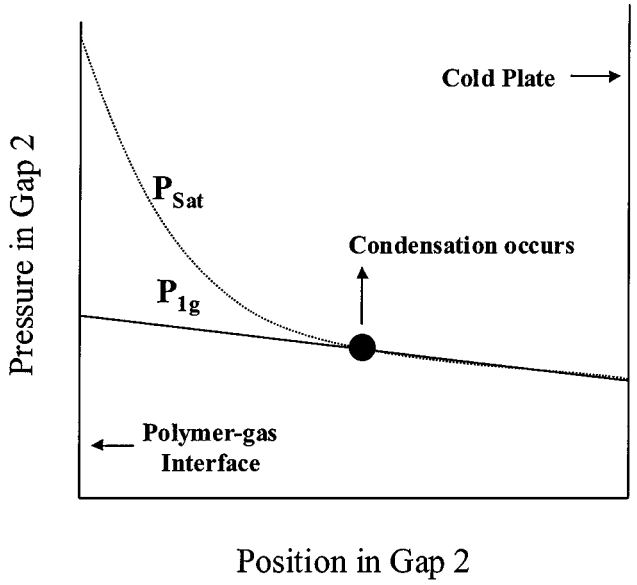


**Figure 3. Occurrence of condensation.**

The solid line represents the partial pressure as a function of the position in gap 2. The dotted line indicates the saturation pressure in gap 2, determined from the temperature profile, as a function of position. When the saturation pressure equals the saturation pressure, that is, when the solid and dotted lines intersect, condensation occurs.

cult problem to eliminate (Fair et al., 1984). In fact, it seems the only way to counteract this tendency for the heat-transfer process to be faster than the mass-transfer process is to introduce a higher energy load on the heat-transfer process. For example, if thermal energy could be supplied to the vapor in gap 2, this would help eliminate the intersection of the vapor-pressure curve and the saturation-pressure curve in the gap. One possible way to achieve such a modification would be to place a thin metal screen in gap 2, and by passing an electrical current through this screen one could heat it up and therefore modify the temperature gradient in the gap. Figure 4 shows the temperature gradient in the upper gap, which has been modified by incorporation of a heated screen. The heated screen provides thermal energy to the gas phase in addition to the energy supplied by the lower hot plate. In addition to the temperature of the screen, the placement in gap 2 is another variable that can be manipulated to prevent condensation in the gas phase. It must be noted that in the analysis of the problem with a screen in gap 2, it is assumed that the screen does not physically interfere with the mass-transfer process, while the temperature gradients and concentrations in the gas phase are modified because of the additional energy supplied by the screen.

To investigate the influence of the placement of a heated screen in gap 2 on the drying process (Case B), as well as the premature condensation phenomenon, the gap-dryer model was modified to incorporate the influence of a heated screen. Mathematically, the heated screen is treated as a line source of thermal energy that is maintained at a constant temperature. In addition to the base-line case (Case A), which is represented by Figure 2, four other cases were considered in order to evaluate the influence of the heated-screen concept. The data and parameters presented in Table 1 are common

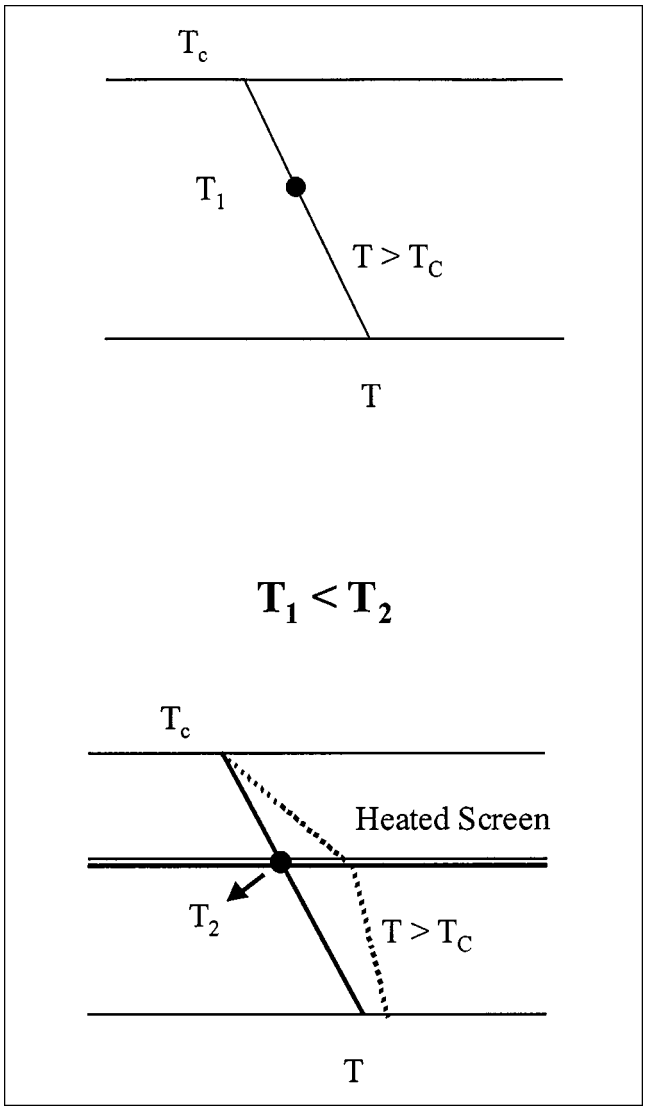


**Figure 4. Heated screen placed in gap 2 alters the temperature gradients and prevents condensation.**

The solid line indicates the temperature profile in the absence of a heated screen, while the dotted line indicates the temperature profile when a heated screen is present.

to all the cases considered. Further specific conditions for the various cases are presented in Table 2.

The influence of a heated screen in gap 2 (Case B) on the overall drying process is shown in Figure 5. This figure shows the drying curve (average concentration vs. time and temperature vs. time) in the coating for the unmodified gap dryer (Case A) operating under the conditions presented in Table 2, as well as the drying curve for a gap dryer that was modified with a heated screen. The results presented in Figure 5 are for the case where the heated screen is placed a distance of one-tenth the gap-2 thickness from the cold plate and maintained at a temperature of 315 K. The model simulation for this case indicates that the presence of the heated screen will eliminate condensation in the gas phase, and in addition, the drying rate is improved somewhat. The improvement in

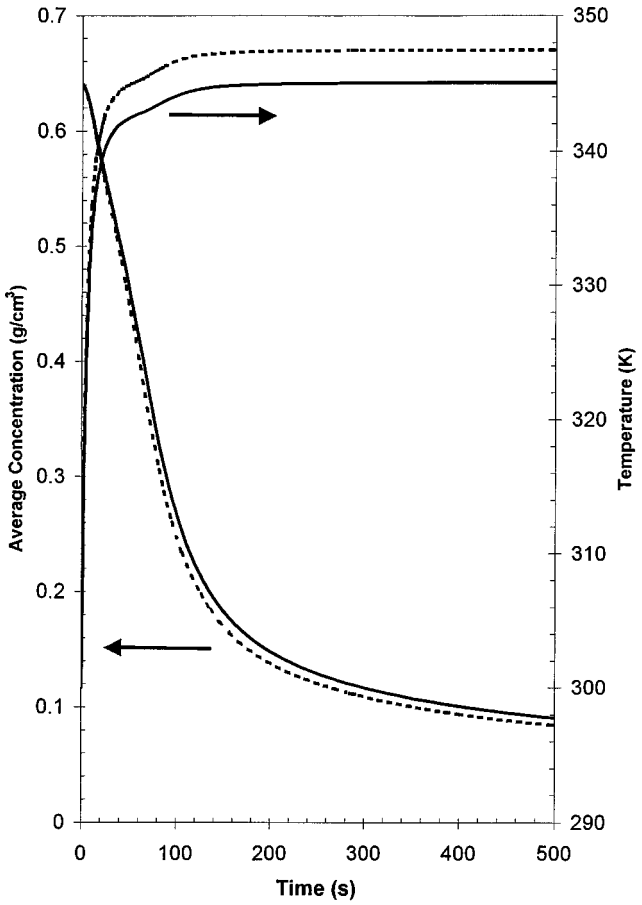


**Figure 5. Comparison of drying curves (average concentration vs. time and temperature vs. time) for a gap dryer with and without a heated screen for the PVAC–toluene system.**

Dark solid line represents Case A, while the broken line represents Case B.

the drying rate is due to the modification of the relative resistance in gap 2 resulting from the additional heat supplied by the heated screen. This change in relative resistances increases the temperature at the polymer–gas interface, and consequently the rate of evaporation. The increased interfacial temperature is qualitatively illustrated in Figure 4, and the actual temperature of the coating with the screen present in gap 2 is illustrated in Figure 5, from which it is clear that higher values of temperature are attained at long times.

Obviously, one of the drawbacks of placing the heated screen in gap 2 is that the load on the cold plate is increased. Also, since the gap is extremely small, it may be difficult to place a screen in a gap of such dimensions and maintain space between the screen and the polymer film at all positions in the dryer. The incorporation of a heated screen may require increasing the gap size in such a dryer.

A third simulation of the gap dryer for the toluene–PVAC system was conducted maintaining all the conditions presented in Table 2, with the exception that gap 2 is increased from 0.16 cm to 0.35 cm (Case C). Rayleigh number calculations indicate that even with this increased gapwidth, natural convection will still not be important. In addition to the increase in the gapwidth, the screen temperature had to be increased to 325 K to prevent solvent condensation in the gas phase. As in the previous case, the screen was placed at a distance of one-tenth the gap width from the upper cold plate. A comparison of Cases B and C is presented in Figure 6. It is clear that increasing the dimensions of the gap increases the gas-phase resistance, and therefore decreases the initial rate of drying. Also, as in Case B, the increase in the dimension of gap 2 changes the relative thermal resistance in the two gaps and the coating. As a result, with a larger gap 2 the temperature of the coating attains a higher value, as shown in Figure 6. This is reflected in the slightly lower residual amount of solvent in the coating at large times ($t > 200$ s). There are obviously several combinations of screen position and screen temperature that could be used to eliminate undesirable condensation. As the screen is moved away from the cold plate, the temperature of the screen must be increased. Further, it must be noted that there always exists a small zone adjacent to the cold plate where precondensation may occur. This zone can be made smaller by increasing the temperature of the screen until condensation practically occurs at the cold plate.

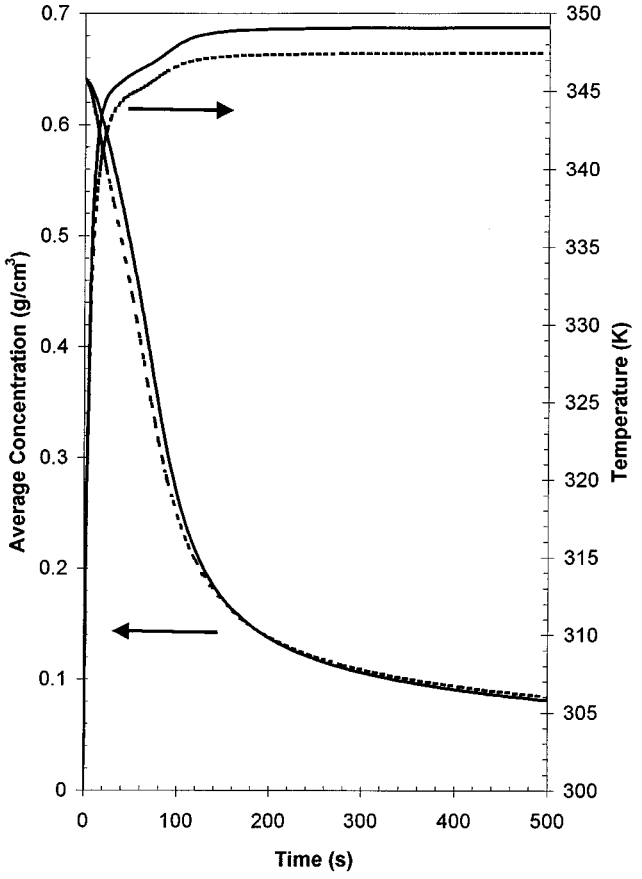


**Figure 6. Effect of increasing dimensions of gap 2 on the drying curve (average concentration vs. time and temperature vs. time) in a gap dryer with a screen for the PVAC–toluene system.**

Dark solid line represents Case C, while the broken line represents Case B.

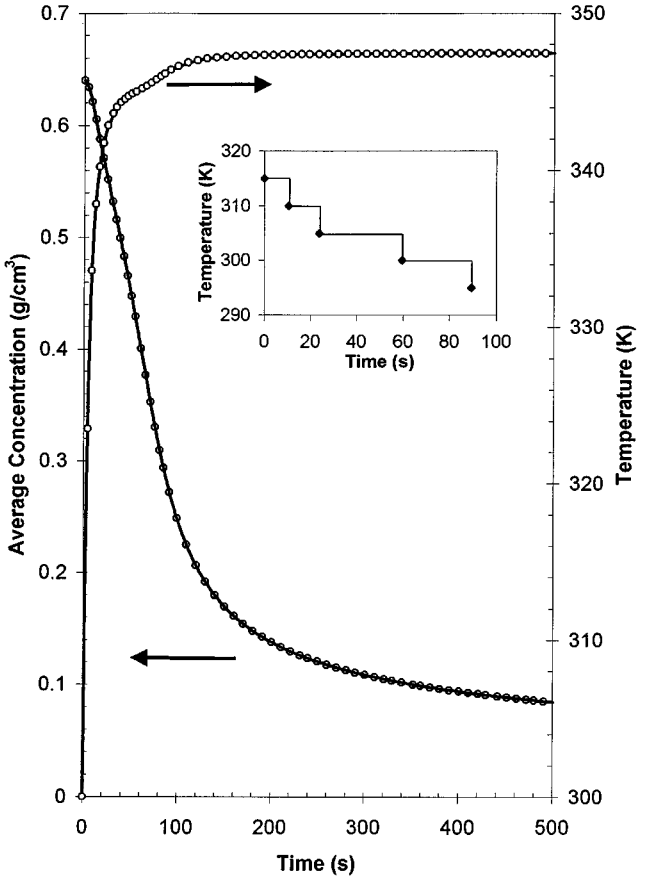


**Figure 7. Effect of varying the temperature in gap 2 as a function of time on the drying curve (average concentration vs. time and temperature vs. time) in a gap dryer with a screen for the PVAC–toluene system.**

Solid line represents Case B, while symbols represent Case D.

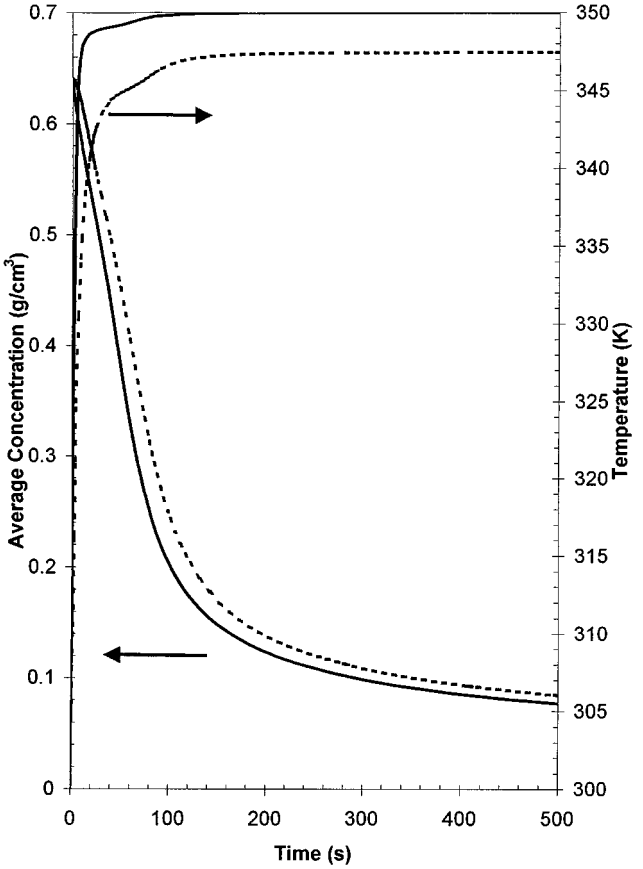


**Figure 8. Comparison of drying (average concentration vs. time and temperature vs. time) in a gap dryer and convection oven dryer.**

The parameters for generating the curve for the convection oven dryer are given in Table 3. Dark solid line represents the convection dryer, while the broken line represents Case B.

Increasing the temperature of the screen will, of course, have a beneficial effect on the drying process; however, the load on the cold plate would also increase, perhaps offsetting the beneficial effects of quicker drying.

The heated screen is not required for the entire duration of the drying process. After the initial phase where gas-phase mass transfer controls the drying process, the activity of the solvent at the polymer–gas interface becomes significantly lower, and the temperature of the screen required to eliminate precondensation can be reduced. This is highly desirable, since this will also reduce the cooling load on the cold plate. As in the case of conventional forced-convection dryers, one can envision the gap dryer having different zones with different temperatures on the plates and on the screen.

An analysis of a gap dryer with several zones dictated by the temperature of the heated screen was conducted as Case D. All the conditions for Case D were equivalent to those for Case B, except that the temperature of the screen was varied along the gap dryer, as indicated on the insert in Figure 7. This figure also shows a comparison of the drying curves (average concentration vs. time and temperature vs. time) for Cases B and D. It is obvious from this analysis that changing the temperature of the screen does not have a discernable effect on the drying process.

Finally, the drying curve for the gap dryer is compared with the drying characteristics of a conventional convection-oven dryer in Figure 8. In this figure, the gap-dryer behavior is represented by Case B, and the forced-convection drying curve is based on parameters that are typical of those realized in industrial dryers, as presented by the analysis of Alsoy and Duda (1998). The parameters used in the simulation are listed in Table 3. Although a direct comparison is impossible since the configurations and parameters in the two dryers are different, Figure 8 indicates that the drying rate obtained in the gap dryer, while lower than the convection dryer for the conditions chosen (owing to higher mass-transfer coefficients obtainable in the convection dryer), is still comparable. Also, the gradients in concentration that exist in the convection dryer are extremely sharp, and could cause skinning. It must also be noted that the temperature of the coating attainable in a convection-oven dryer is higher than in a gap dryer, since the coating is in direct contact with the heated air. Obviously, the drying rate in a gap dryer could be increased by decreas-

**Table 3. Drying Parameters for PVAC-Toluene System in a Convection Dryer**

| Parameters for Drying Simulation | Values |
|---|---|
| *Initial conditions* | |
| Temperature | 300 K |
| Coating thickness | 0.0254 cm |
| Initial concentration of the solvent | 0.64 g/cm$^3$ |
| *Substrate Parameters* | |
| Heat capacity | 1.25 J/g·K |
| Density | 1.37 g/cm$^3$ |
| Base thickness | 0.0508 cm |
| *Coating Parameters* | |
| Heat capacity | 1.65 J/g·K |
| Density | 1.18 g/cm$^3$ |
| Heat of vaporization | 360 J/g |
| *Operating Conditions* | |
| Base-side heat-transfer coefficient | 0.039 W/cm$^2$·K |
| Coating-side heat-transfer coefficient | 0.039 W/cm$^2$·K |
| Bottom air supply temperature | 350 K |
| Top air supply temperature | 350 K |
| Mass-transfer coefficient | $5.92\times10^{-8}$ s/cm |

ing the temperature of the cold plate, which would increase the driving force for mass transfer in the gas phase.

In addition to the possible formation of liquid droplets in the gas phase, which is unique to the gap dryer, a change of phase can occur in the polymeric phase for both dryers. If the partial pressure of the solvent in the polymer phase becomes greater than the atmospheric pressure, nucleation can occur and bubbles that lead to defects are produced. Detailed analysis of the conditions in the polymer phase indicate that the partial pressure of the solvent is less than atmospheric pressure in the polymer phase for all the cases considered in this analysis of the gap dryer. Bubble formation can also be related to the solubility of dissolved air in the polymer phase. This phenomenon was not accounted for in this study.

In commercial forced-convection dryers, the velocity of the air over the polymer phase causes enhancement of heat and mass transfer in the gas phase. The model for the gap dryer would have to be modified if the velocity of the conveyer is high enough to significantly influence heat and mass transfer in the two gaps. Correlations for heat and mass transfer in the gas phase indicate that velocities as high as 1 cm/s in the gap dryer will not cause significant enhancements in the gap. Higher velocities will enhance the heat and mass-transfer rates, and may aggravate the condensation problem, since solvent vapor will be convected to regions of lower temperature. The placement of a screen in gap 2 will reduce the convection currents and may prove to be an effective solution to this problem caused by an enhanced rate of mass transfer.

## Conclusions

A mathematical model has been developed to describe the coupled heat and mass transfer in a gap dryer. These model equations have been solved to investigate the drying of the solution of polyvinyl acetate and toluene under conditions that are typical for commercial drying operations. The drying curves, or the concentration of the solvent in the polymer phase as a function of time in the dryer, and temperature of the coating as a function of time, show similar behavior as that exhibited by conventional forced-convention dryers.

Closer examination of the model results indicate, however, that the gap dryer has a unique problem that is not encountered in conventional forced-convection drying processes. Under most conditions that would be characteristic of conventional drying operations, the solvent vapor pressure in the upper gap of the dryer becomes larger than the saturation vapor pressure. Consequently, it is very likely that condensation or solvent fog will be formed in the upper gap of the gap dryer. Furthermore, it seems possible that these liquid droplets will rain down upon the evaporating polymer solution and not only reduce the drying efficiency, but can very possibly lead to surface defects on the resulting polymer film.

This premature vapor-phase condensation is a fundamental problem that is related to the fact that the heat transfer in the gas phase is always faster than the mass transfer and cannot be eliminated by adjustment of the drying conditions if the efficiency of the gap dryer is to be maintained. A modification of the gap dryer is proposed that can potentially eliminate this problem. It is shown that the placement of a thin heated screen in gap 2 can increase the thermal load through the heat-transfer process, and consequently eliminate this precondensation or supersaturation condition. While this alleviates the problem of condensation in the gap, it places an additional load on the cold plate. It is also shown that a screen need not be operational at the highest temperature throughout the drying process, and that its temperature can be reduced as the drying process proceeds. Consequently, this is equivalent to running the gap dryer with several temperature zones. While this procedure reduces the load on the cold plate, the analysis indicates that it does not have a significant effect on the overall drying rate for the chosen conditions. In order to obtain optimal drying conditions, while at the same time eliminating the premature condensation, a rigorous constrained optimization approach would have to be adopted. The influence of the placement of the screen and the temperature of the screen are two variables that need to be studied in greater detail. While exclusion of the radiation term may not cause a significant change in drying rates observed at low temperatures, it may be a factor that influences drying considerably at higher temperatures. In addition, radiation also places a greater load on the cooling system.

It should be emphasized that the utilization of a heated screen has been shown to work in theory, but the actual incorporation of such a heating element in a very narrow gap may not be practically possible. Although the premature condensation in the gap is a problem that must be addressed, this analysis does show that the gap dryer can be used to effectively form polymer coatings and films in a manner comparable to convection of a dryer. In addition, a gap dryer has several advantages from the point of view of solvent recovery and the alleviation of enviromental concerns related to potential air pollution associated with the hydrocarbon solvents.

## Literature Cited


Alsoy, S., and J. L. Duda, ''Drying of Solvent Coated Polymer Films,'' *Drying Tech.*, **16**, 15 (1998).

Blandin, H. P., J. C. David, and J. M. Vergnaud, ''Modeling of Drying of Coatings: Effect of Thickness, Temperature and Concentration of Solvent,'' *Prog. Org. Coatings*, **15**, 163 (1987).

Cairncross, R. A., L. F. Francis, and L. E. Scriven, ''Competing Drying and Reaction Mechanisms in the Formation of Sol to Gel Films, Fibers and Spheres,'' *Drying Tech.*, **10**, 893 (1992).

Cairncross, R. A., S. Jeyadev, R. F. Dunham, K. Evans, L. F. Francis, and L. E. Scriven, ''Modeling and Design of an Industrial Dryer with Convective and Radiant Heating,'' *J. Appl. Poly. Sci.*, **58**, 1279 (1995).

Daubert, T. E., and R. P. Danner, *Physical and Thermodynamical Properties of Pure Compounds: Data Compilation*, Taylor & Francis, New York (1994).

Fair, J. R., D. E. Steinmeyer, W. R. Penney, and B. B. Crocker, ''Liquid-Gas Systems,'' *Perry's Chemical Engineers Handbook*, 6th ed., Chap. 18, D. W. Green, and J. O. Maloney eds., p. 55 (1984).

Hong, S.-U., ''Molecular Diffusion of Organic Solvents in Multicomponent Polymeric Materials,'' PhD Thesis, Pennsylvania State Univ., University Park (1994).

Huelsman, G. L., and W. B. Kolb, ''Coated Substrate Drying System,'' U.S. Patent No. 5,694,701 (1997).

Kolb, W. B., and G. L. Huelsman, ''Gap Drying: An Overview,'' *Proc. Int. Coating Sci. and Tech. Symp. Conf.*, 209 (1998).

Okazaki, M., K. Shioda, K. Masuda, and R. Toei, ''Drying Mechanism of Coated Film Polymer Solution,'' *J. Chem. Eng. Jpn.*, **7**, 99 (1974).

Price, P. E., Jr., S. Wang, and I. H. Romdhane, ''Extracting Effective Diffusion Parameters from Drying Experiments,'' *AIChE J.*, **43**, 1925 (1997).

Vrentas, J. S., and J. L. Duda, ''Diffusion in Polymer-Solvent Systems—I. Re-examination of the Free-volume Theory,'' *J. Poly. Sci.: Part B: Poly. Phys.*, **15**, 403 (1977a).

Vrentas, J. S., and J. L. Duda, ''Diffusion in Polymer-Solvent Systems: II. A Predictive Theory for the Depenence of Diffusion Coefficients on Temperature, Concentration and Molecular Weight,'' *J. Poly. Sci.: Part B: Poly. Phys.*, **15**, 417 (1977b).

Vrentas, J. S., and C. M. Vrentas, ''Drying of Solvent Coated Polymer Films,'' *J. Poly. Sci.: Part B: Poly. Phys.*, **32**, 187 (1994a).

Vrentas, J. S., and C. M. Vrentas, ''Solvent Self-Diffusion in Rubbery Polymer-Solvent Systems,'' *Macromol.*, **27**, 4684 (1994b).

Vrentas, J. S., and C. M. Vrentas, ''Predictive Methods for Self-Diffusion and Mutual Diffusion Coefficients in Polymer-Solvent Systems,'' *Eur. Poly. J.*, **34**, 797 (1998).

Yapel, R. A., ''The Physical Model of Drying of Coated Films,'' MS Thesis, Univ. of Minnesota, Minneapolis (1988).

Waggoner, R. A., and D. F. Blum, ''Solvent Diffusion and Drying of Coatings,'' *J. Coatings Tech.*, **61**, 51 (1989).

Zielinski, J. M., ''Free Volume Parameter Estimation for Polymer-Solvent Diffusion Coefficient Predictions,'' PhD Thesis, Pennsylvania State Univ., University Park (1992a).

Zielinski, J. M., and J. L. Duda, ''Predicting Polymer-Solvent Diffusion Coefficients Using Free-Volume Theory,'' *AIChE J.*, **38**, 405 (1992b).

*Manuscript received May 15, 2000, and revision received Oct. 31, 2000.*